17. Noguchi M, Morikawa A, Kawasaki M, et al: Small adenocarcinoma of the histologic characteristics and prognosis. Cancer 75:2844-2852, 1995

18. Kodama K, Doi O, Higashiyama M, et al: Intentional limited resection for selected patients with T1 N0 M0 non-small-cell lung cancer: A single-institution study. J Thorac Cardiovasc Surg 114:347-353, 1997

19. Ginsberg RJ, Rubinstein LV: Randomized trial of lobectomy versus limited resection for T1N0 non-small cell lung cancer: Lung Cancer Study Group. Ann Thorac Surg 60:615-622, 1995

20. Sobue T, Ajiki W, Tsukuma H, et al: Trends of lung cancer incidence by histologic type: A population-based study in Osaka, Japan. Jpn J Cancer Res 90:1-10, 1999

21. Sobue T, Suzuki T, Fujimoto I, et al: Lung cancer risk among exsmokers. Jpn J Cancer Res 82:273-279, 1991

22. Sobue T, Suzuki T, Fujimoto I, et al: Case-control study for lung cancer and cigarette smoking in Osaka, Japan: Comparison with the results from Western Europe. Jpn J Cancer Res 85:464-473, 1994

Progression of Focal Pure Ground-Glass Opacity Detected by Low-Dose Helical Computed Tomography Screening for Lung Cancer

Ryutaro Kakinuma, MD, Hironobu Ohmatsu, MD, Masahiro Kaneko, MD, Masahiko Kusumoto, MD, Junji Yoshida, MD, Kanji Nagai, MD, Yutaka Nishiwaki, MD, Toshiaki Kobayashi, MD, Ryosuke Tsuchiya, MD, Hiroyuki Nishiyama, MD, Eisuke Matsui, MD, Kenji Eguchi, MD, and Noriyuki Moriyama, MD

Objective: To clarify the progression of focal pure ground-glass opacity (pGGO) detected by low-dose helical computed tomography (CT) screening for lung cancer.

Methods: A total of 15,938 low-dose helical CT examinations were performed in 2052 participants in the screening project, and 1566 of them were judged to have yielded abnormal findings requiring further examination. Patients with peripheral nodules exhibiting pGGO at the time of the first thin-section CT examination and confirmed histologically by thin-section CT after follow-up of more than 6 months were enrolled in the current study. Progression was classified based on the follow-up thin-section CT findings.

Results: The progression of the 8 cases was classified into 3 types: increasing size (n = 5: bronchioloalveolar carcinoma [BAC]), decreasing size and the appearance of a solid component (n = 2: BAC, n = 1; adenocarcinoma with mixed subtype [Ad], n = 1), and stable size and increasing density (n = 1: BAC). In addition, the decreasing size group was further divided into 2 subtypes: a rapid-decreasing type (Ad: n = 1) and a slow-decreasing type (BAC: n = 1). The mean period between the first thin-section CT and surgery was 18 months (range: 7–38 months). All but one of the follow-up cases of lung cancer were noninvasive whereas the remaining GGO with a solid component was minimally invasive.

Conclusions: The pGGOs of lung cancer nodules do not only increase in size or density, but may also decrease rapidly or slowly with the appearance of solid components. Close follow-up until the appearance of a solid component may be a valid option for the management of pGGO.

Key Words: ground-glass opacity, low-dose helical computed tomography screening, lung cancer

(*J Comput Assist Tomogr* 2004;28:17–23)

Focal pure ground-glass opacities (pGGOs), or nodules of the lungs, has become a major concern as low-dose helical computed tomography (CT) screening for lung cancer becomes more widely available, not only in the field of diagnostic imaging,[1–5] but also in the field of limited surgery.[6–10] GGO is a finding on thin-section CT images of the lung which has been described as a hazy, increased attenuation of the lung tissue with preservation of the bronchial and vascular margins. GGO is usually a nonspecific finding that is found in many types of pulmonary disease.[11] However, some investigators have recently reported that most localized pGGOs or focal GGOs are malignant.[1,2,5] Although a few reports have described the evolution of lung cancer using conventional chest CT,[12–14] thin-section CT[15–17] and low-dose screening CT,[18,19] the natural history of peripheral lung cancers that exhibit as pGGO on thin-section CT images detected using low-dose helical CT screening is still unclear.

The purpose of this retrospective study was to clarify the progression of pGGOs, which were not visible on chest radiographs, detected by low-dose helical CT screening examinations performed every 6 months. We evaluated the progression of pGGOs based on the thin-section CT findings obtained during the follow-up after the first thin-section CT.

PATIENTS AND METHODS

Subjects

Between September 1993 and January 2003, low-dose helical CT screening was conducted semiannually in Tokyo by

From the Division of Thoracic Oncology (Drs Kakinuma, Ohmatsu, Yoshida, Nagai, and Nishiwaki), National Cancer Center Hospital East, Tsukiji, Chiba Japan; the Divisions of Endoscopy (Drs Kaneko and Kobayashi), Diagnostic Radiology (Drs Kusumoto and Moriyama), and Thoracic Surgery (Dr Tsuchiya), National Cancer Center Hospital; the Division of Thoracic Surgery (Dr Nishiyama), Social Health Insurance Medical Center, Okubo, Japan; (Dr Matsui); the Anti–Lung Cancer Association, Ichigaya, Japan; and the Division of Internal Medicine (Dr Eguchi), School of Medicine, Tokai University, Isehara, Japan.

This study was supported in part by a Grant-in-Aid for Cancer Research (13-8) from the Ministry of Health, Labor, and Welfare of Japan and by a Grant-in-Aid from the Second-Term Comprehensive 10-Year Strategy for Cancer Control.

Reprints: Ryutaro Kakinuma, MD, National Cancer Center Hospital East, 6-5-1 Kashiwa-no-ha, Kashiwa, Chiba 277-8577, Japan (e-mail: rkaki@east.ncc.go.jp).

the Anti–Lung Cancer Association (ALCA), a for-profit organization for lung cancer screening.[20,21] Each screening consisted of a low-dose helical CT examination, chest radiography, and cytologic sputum studies. During this period, a total of 15,938 low-dose helical CT examinations were performed in 2052 ALCA members. Among the low-dose helical CT examinations, a total of 1566 CT examinations were judged as having abnormal findings requiring further examination. Sixty-seven cases of lung cancer (peripheral-type lung cancer, 61; hilar-type lung cancer, 6) were detected during the ALCA lung cancer screening project. Out of these 67 cases, 51 cases (76%) were pathologic stage IA. The treatments used in the 67 cases were as follows: surgery (n = 55), radiotherapy (n = 5), radiotherapy and chemotherapy (n = 2), chemotherapy (n = 4), and photodynamic therapy (n = 1). Among the patients with peripheral nodules detected by the low-dose helical CT examinations performed every 6 months, the patients with histologically diagnosed nodules exhibiting pGGO larger than 5 mm in diameter at the time of the first thin-section CT and followed-up by thin-section CT for more than 6 months were enrolled in the current study.

CT Scanning Conditions

A TCT900S Superhelix CT scanner (Toshiba Medical Inc., Tokyo, Japan) was used for all of the examinations. Low-dose helical CT screening was performed under the following conditions: 120 kV, 50 mA, beam width of 10 mm, 1 rotation of the x-ray tube per second, and a table speed of 20 mm per second (pitch 2:1). Reconstruction was performed at intervals of 10 mm. The CT images were displayed on a monitor with a window width of 2000 HU and a window level of −700 HU. If newly developed nodules were identified, thin-section CT examinations were performed under the following conditions: 120 kV, 250 mA, beam width of 2 mm, 1 rotation of the x-ray tube per second, and a table speed of 2 mm per second (pitch 1:1). Reconstruction was performed at intervals of 2 mm using a thin-section CT algorithm.

Evaluation of pGGO Progression Patterns

The progression patterns were classified based on changes in the size and density of the pGGOs on the thin-section CT images. The study period was divided into 2 phases: the unidentified phase (ie, the period prior to the first thin-section CT scan) and the follow-up phase (ie, the period after the first thin-section CT scan). CT images of the pGGOs in the unidentified phase were reviewed independently by 4 physicians (R.K., M.K., H.O., K.E.), who are diagnostic experts in chest radiology, and by 1 radiologist (M.K.). CT findings were adopted as positive findings if 3 of more of the doctors agreed. After the independent reviews, we decided by consensus as to how many pGGOs were newly developed or had arisen from inconspicuous nodules during the helical CT screening period. In the follow-up phase, the size of the pGGOs was measured with a pair of calipers on the thin-section CT images obtained during the initial scan and the final scan by consensus of 2 diagnostic experts (R.K., M.K.) to assess doubling time. The size of the lesion was evaluated using measurements that passed through the center of the lesion. Size was defined as the average of the length and width of the lesion. Doubling times were calculated using the Schwartz equation.[22] The density of faint opacities was evaluated visually on the thin-section CT images obtained during the follow-up phase. pGGO was defined as a homogeneous GGO, and mixed GGO was defined as a GGO with a solid component.

Pathologic Classification of Adenocarcinomas

The histologic findings of the adenocarcinomas were classified according to the criteria of the World Health Organization (WHO)[23] and the criteria of Noguchi et al.[24] The classification system for replacement growth patterns developed by Noguchi et al is as follows: type A (localized bronchioloalveolar carcinoma; LBAC), type B (LBAC with foci of collapsed alveolar structure), and type C (LBAC with foci of active fibroblastic proliferation).

RESULTS

Patient Characteristics

Eight patients with pGGOs (6 men and 2 women) were enrolled in the current study (Table 1). The patients ranged in age from 49 to 69 years (mean, 64 years). With regard to smoking history, 3 patients were nonsmokers, 4 were ex-smokers, and 1 was a current smoker. Four of these 8 pGGO patients were not apparent during the initial screening and became apparent during the screening period, and 3 of the other 4 pGGO patients with inconspicuous opacities visible in retrospect during the initial screening became apparent later. In 1 other case, a conspicuous opacity and multiple old tuberculosis lesions were observed during the initial CT screening. The locations of the pGGOs were as follows: right upper lobe (n = 4), right lower lobe (n = 1), left upper lobe (n = 1), and left lower lobe (n = 2).

Clinical Course

The period between the first visible nodule of a pGGO on a thin-section CT image and the first visible opacity on a helical CT screening image when viewed retrospectively ranged from 13 to 46 months (mean, 22 months) (Table 1). The period between the first thin-section CT examination and the surgery ranged from 7 to 39 months (mean, 19 months). The interval between the last thin-section CT examination and surgery ranged from 1 to 98 days (mean, 32 days).

Histology of GGOs

Seven patients had bronchioloalveolar carcinoma (BAC), defined as noninvasive by the WHO classification in 1999, and 1 had an adenocarcinoma with mixed subtypes (Table 1). Based on Noguchi's classification for small adeno-

TABLE 1. Clinical Characteristics and Histology of Ground-Glass Opacities

Case No.	Sex	Age at Detection (Years)	Smoking Index	Development	Lobe	Period Between: First Visible and the First TS-CT (Months)*	Period Between: The First TS-CT and Surgery (Months)*	Period Between: The Last TS-CT and Surgery (Days)	Histology: WHO Classification	Histology: Noguchi Type
1	M	69	1300	New	RU	41	13	1	Ad	C
2	M	69	800 (ex)	New	RU	13	39	36	BAC	B
3	F	66	Non	New	LL	13	14	33	BAC	A
4	M	66	450 (ex)	New	LU	18	26	98	BAC	A
5	F	65	Non	ic	LL	46	28	13	BAC	B
6	M	69	800 (ex)	ic	RU	21	12	13	BAC	A
7	M	49	515 (ex)	ic	RU	14	10	6	BAC	A
8	M	63	Non	c	RL	13	7	57	BAC	B

Non, nonsmoker; ex, ex-smoker; ic, inconspicuous; c, conspicuous; RU, right upper lobe; LU, left upper lobe; LL, left lower-lobe; TS-CT, thin-section CT; BAC, bronchioloalveolar carcinoma; Ad, adenocarcinoma.
*Number of months was rounded.

carcinomas, the pGGOs consisted of 4 cases of type A and 2 cases of type B while the mixed GGOs consisted of 1 case of type B and 1 case of type C (Tables 1, 2). All the lung cancers were diagnosed at pathologic stage IA.

Progression of pGGOs

The period between the first thin-section CT and the final thin-section CT examinations ranged from 6 to 37 months (mean, 17 months) (Table 3). The opacities ranged in size from 6.5 mm to 17 mm (mean, 10 mm) at the time of the first thin-section CT examination and from 7 mm to 16.5 mm (mean, 10.5 mm) at the time of the final thin-section CT examination. The progressions of 8 opacities in the follow-up phase were classified into 3 types: increasing in size (Increasing type, n = 5), decreasing in size and the appearance of a solid component (decreasing type, n = 2), and stable in size and increasing in density (density type, n = 1). In addition, the decreasing type was classified into 2 subtypes: a rapid-decreasing type (case 1, Fig. 1; decrease in size at the time of the 6-month follow-up) and a slow-decreasing type (case 2, Fig. 2; decrease after follow-up for more than 1 year). All but 1 of the follow-up cases were noninvasive, and the remaining GGO with a solid component was judged to be minimally invasive adenocarcinoma because the size of the collapse fibrosis was only 2 mm in diameter (Fig. 1F).

TABLE 2. Thin-Section CT Findings, Progression Types, and Doubling Time of Ground-Glass Opacities

Case No.	Follow-Up Phase with Thin-Section CT: GGO Size (mm) First	GGO Size (mm) Final	Final TS-CT of GGO: Density	Solid	Finding	Progression Type	Period of Follow-Up with TS-CT (Months)*	GGO Doubling Time (Days)
1	17	12	Increasing	+	Mixed	Dec	12	−214
2	14	12	Increasing	+	Mixed	Dec	37	−1680
3	6.5	7.5	Stable	−	Pure	Inc	13	617
4	7	10.5	Stable	−	Pure	Inc	22	383
5	7	7	Increasing	−	Pure	Den	27	—
6	8.5	9.5	Stable	−	Pure	Inc	12	669
7	6.5	9	Stable	−	Pure	Inc	10	216
8	13.5	16.5	Stable	−	Pure	Inc	6	198

CT, computed tomography; GGO, ground-glass opacity; TS-CT, thin-section computed tomography; Inc, increasing; Dec, decreasing; Den, density.
*Number of months was rounded.

TABLE 3. Evolution of Solid Components in Ground-Glass Opacities

Case No.	Follow-Up Phase with TS-CT Solid Size (mm)					Doubling Time (Days)
	First TS-CT	Months After the First TS-CT				
		6	11	23	36	
1	0*	8				14*
2	0	—	2	3	7.5	130†

TS-CT, thin-section computed tomography.

*Doubling time of solid component in case 1 was calculated on the assumption that the first size was 0.5 mm.

†Doubling time of solid component in case 2 was calculated based on the sizes between 11 months and 36 months after the first TS-CT.

Doubling Time

The doubling times of the increasing-type opacities ranged from 198 to 669 days (mean ± SD, 417 ± 220 days). The doubling time of the density-type opacity could not be calculated because it did not change in size. For the decreasing-type opacities, the doubling times were calculated based on the sizes of the pGGOs and the solid components, individually. In case 1, the doubling times of the pGGO and the solid component were −214 and 14 days, respectively. In case 2, the doubling times of the pGGO and the solid component were 1680 and 130 days, respectively.

Correlation of Thin-Section CT Images and Pathologic Findings

The pGGO corresponded to the lepidic growth of cancer cells (Fig. 1E), the thickening of the alveolar wall (Fig. 1E), and the collapse of the alveolar space (Fig. 1E). Solid components corresponded not only to the collapse of the alveolar space and fibrosis (Fig. 1F and Fig. 2G), but also to a severe narrowing of the alveolar space (Fig. 1F). With the development of a solid component in case 2, the distance between the surrounding pulmonary veins and the bronchus gradually narrowed (Figs. 2C–F). The same finding was observed in case 1 (Figs. 1C, D).

DISCUSSION

To our knowledge, this study is the first report to describe the progression of pGGOs in minute lung cancers that appeared as new pGGOs during the screening process or arose from inconspicuous minute nodules on low-dose helical CT screening images obtained at 6-month intervals. In addition, the progressions of the pGGOs on the thin-section CT images were classified into 3 types for the first time. Although a few papers have described the natural history of GGOs in pulmonary adenocarcinoma,[4,7,12,15–17] only 1 researcher[15] reported 2 GGOs that decreased in size, but the size reduction occurred in mixed GGOs, not in pGGOs. The rapid decreasing of a pGGO and the appearance of a solid component has not previously been reported.

Radiologic-pathologic correlations revealed that pGGOs on thin-section CT images mainly represent the lepidic growth of adenocarcinomas.[1,3,4,12,15–17] Solid components in the mixed GGOs were caused by the collapse of alveolar spaces or regions of fibrosis[12] and by a severe narrowing of the alveolar space (case 1). The narrowing of the distance between the surrounding pulmonary vessels and the bronchus was caused not only by the collapse of the alveolar space (cases 1 and 2), but also by the development of fibrosis (case 1) in the pGGO lesions. This finding has been termed "vessel convergence."[12,15,17] Based on our observations of the progression from a pure GGO to a mixed GGO in cases 1 and 2, our results also support the stepwise progression of replacement-type adenocarcinoma.[12,15,17]

Although 1 researcher raised serious questions about the concept of 2-year stability implying benignity,[25] pulmonary nodules are generally considered to be benign if they remain the same size or decrease in size over a 2-year observation period.[26,27] However, our results show that stability or reduction in size over a 2-year period does not necessarily indicate benignity. In the case of a pGGO that decreases in size, can the Schwartz equation be applied to a change from a pGGO to a mixed GGO if the area of the GGO decreases? Usually, the Schwartz equation is based on the assumption that constant exponential tumor growth is the basic pattern of neoplastic proliferation.[22] The doubling time for mixed GGOs has been reported to be 457 ± 260 days.[28] However, progression to a mixed GGO in a case where the pGGO decreases in size and a solid component simultaneously appears has not previously been reported. Moreover, the calculation of doubling times for each component in a mixed GGO has never, to the best of our knowledge, been performed prior to the current study. The doubling time for the solid component in case 1 was calculated based on the assumption that the initial size of the solid component was 0.5 mm, this because the thin-section CT images were taken not only by the single-slice CT scanner described above, but by a multislice CT scanner with the imaging parameters set at 0.5 mm × 4 rows and image reconstruction performed at 1-mm intervals.

Whether pGGOs should be resected or followed up is controversial. Definite evidence of the natural history of pGGOs does not exist at present. However, based on the indirect corroboration described below, we suggest that close follow-up until the appearance of a solid component may be a valid option for the management of pGGO. First, most pGGOs are either atypical adenomatous hyperplasia (preinvasive lesions according to the 1999 WHO criteria), BAC (a noninvasive lesion), or minimally invasive adenocarcinoma.[1,8,29] Second, 1 researcher[7] has previously reported information concerning

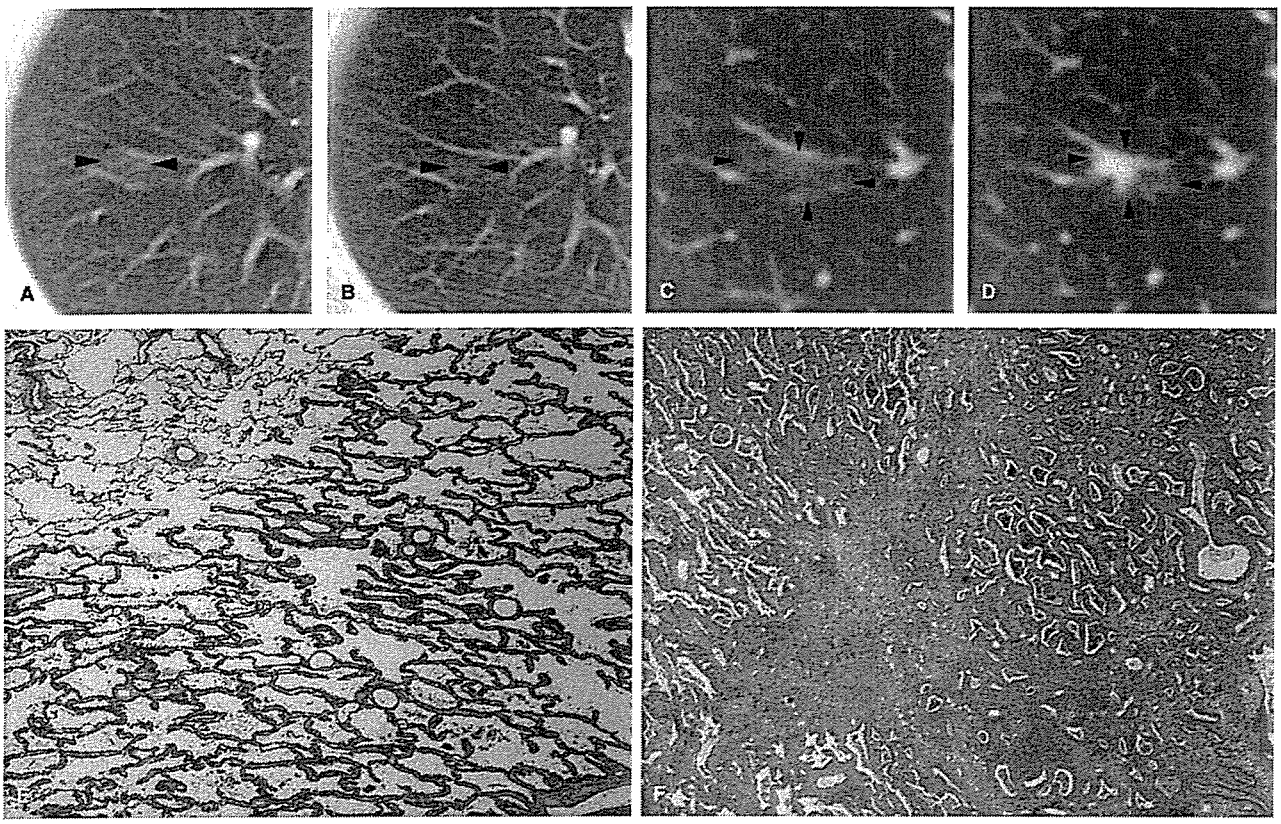

FIGURE 1. Case 1: Adenocarcinoma in a 69-year-old man. A, A faint localized increase in density was identified in segment 1 of the right upper lobe of the lung on a CT screening image obtained in December 2001. B, In retrospect, the opacity was also present on a CT screening image obtained in June 1998. C, Thin-section CT image obtained in December 2001 showing a pGGO in segment 1 of the right upper lobe of the lung. D, Thin-section CT image obtained in June 2002 shows a decrease in the size of the pGGO and the appearance of a solid component. E, Medium-magnification image of the pathologic specimen (H&E staining, ×40). Thickening of the alveolar walls as a result of the tumor cells is visible. F, Medium-magnification image of the pathologic specimen (H&E staining, ×40). Severe narrowing of the alveolar space from the thickening of the alveolar walls and an area of collapse-fibrosis with active fibroblastic proliferation are visible. A right upper lobectomy was performed in January 2003. The lesion was diagnosed as an adenocarcinoma, 17 mm in diameter (Noguchi type C). The size of collapse- fibrosis was 2 mm in diameter.

the natural history of pGGOs after conducting a long-term follow-up study lasting more than 2 years. Five of the 19 cases of pGGOs were diagnosed as lung cancers, that is, 5 BACs (1 case had 2 BACs) and 1 adenocarcinoma, after a mean follow-up of 61 months. Although the patient with adenocarcinoma was followed up for 124 months, personal communication with the author revealed that his lung cancer was of pathologic stage IA and that the size of the central fibrosis of the adenocarcinoma was less than 3 mm in diameter. We have also experienced 2 other pGGOs that developed into mixed GGOs after a 1-year and a 3-year follow-up period, respectively (unpublished data). These lesions were diagnosed as pathologic stage IA adenocarcinomas, and the size of the central fibrosis was 1.5 mm and 2 mm in diameter, respectively. Regarding the relationship between central fibrosis and prognosis, our research team[30] previously reported that 21 out of 100 patients with a lung adenocarcinoma that was 3 cm or less in diameter and which had a central fibrosis of 5 mm or less in diameter had a 5-year survival rate of 100%. Therefore, the adenocarcinoma follow-up cases described above and in this study were thought to be minimally invasive, allowing the possibility of a cure. Third, the adenocarcinoma cases with mixed GGOs did not experience any relapses or deaths, even though the solid components of the GGOs became larger but remained less than 50% of the mixed GGO nodule, this from the standpoint of the GGO's length,[31] the vanishing ratio of GGO[10] ("air-containing type"), and the volume of the GGO.[9] Finally, adenocarcinoma pGGOs tend to grow slowly, as the mean doubling time of pGGOs has been reported to be 813 days[28] or 880 days.[12] In addition, one-fourth of the GGOs in 1 study were

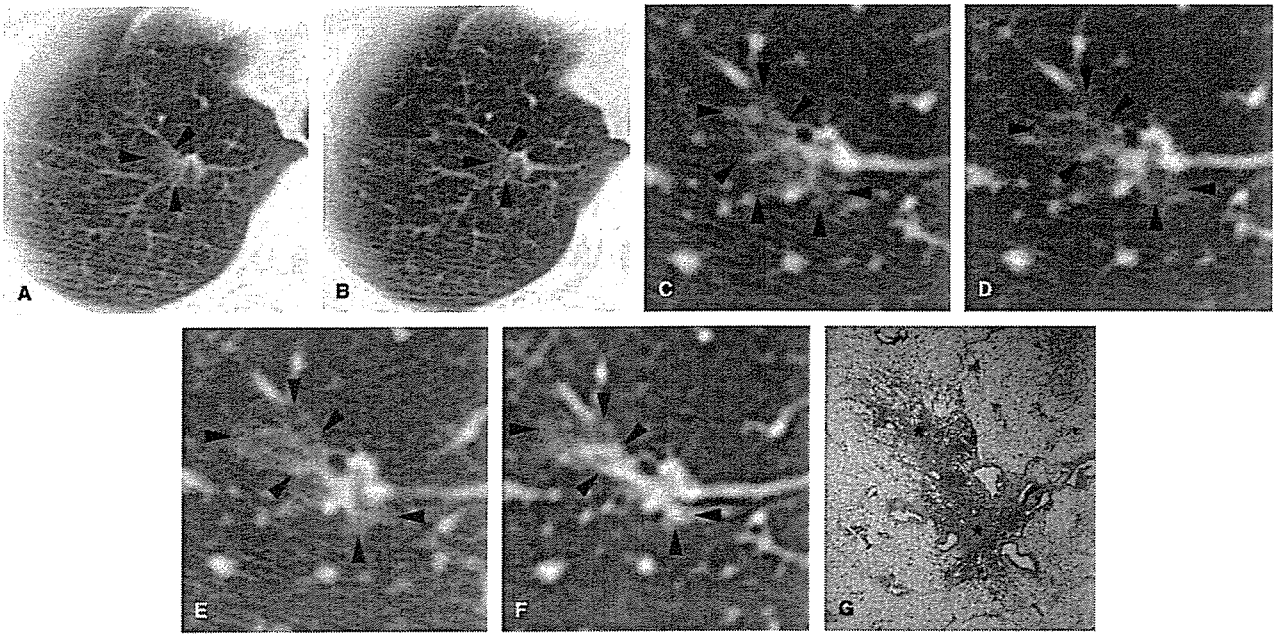

FIGURE 2. Case 2: Bronchioloalveolar carcinoma in a 69-year-old man. A, A faint localized increase in density was identified in segment 1 of the right upper lobe of the lung on a CT screening image obtained in February 1999. B, In retrospect, the opacity was also visible on a CT screening image obtained in February 1998. C, Thin-section CT revealed a pGGO in segment 1 of the right upper lobe of the lung in March 1999. D, Thin-section CT image obtained in February 2000 showing a pGGO with a small solid component. E, Thin-section CT image obtained in February 2001 showing a decrease in the size of the pGGO and a slight increase in the size of the solid component. F, Thin-section CT image obtained in February 2002 showing a larger decrease in the size of the pGGO and an increase in the size of the solid component. G, Low-magnification image of the pathologic specimen (H&E staining, ×5). The foci of alveolar collapse (asterisks) are shown. A right upper lobectomy was performed in May 2002. The lesion was diagnosed as a bronchioloalveolar carcinoma, 15 mm in diameter (Noguchi type B).

stable after a mean follow-up period of 16 months,[17] whereas half of the pGGOs in another study showed no change in size after a median follow-up period of 32 months.[7] Therefore, the classification of some pGGOs may be affected by an overdiagnosis bias.

This study has some limitations. First, the period of pGGO development was not accurately assessed because only thick-sectioned screening CT images were available for the unidentified phase. Therefore, the partial volume effect affected the detectability of small faint opacities on screening CT images. Multislice CT imaging using a narrow collimation and thinner reconstruction images may reveal the natural history of pGGOs more precisely. Second, measurements made with a pair of calipers to calculate doubling times may lead to measurement errors. Although technical advances have been reported,[32,33] we did not have any commercial software for volume measurements. Third, our study cohort was very small. At the start of the helical CT screening project, surgery without follow-up tended to be recommended in cases with pGGO. After knowledge of pGGOs had accumulated (ie, that most pGGOs consisted of preinvasive, noninvasive, or minimally invasive lesions), our treatment procedure changed.[8] Now, resection is only 1 option, not the only option, as in the past. Because of this, resection data cannot always be obtained, and the number of cases was small as a result.

In conclusion, the natural history of pGGOs detected by helical CT screening for lung cancer was partially revealed. A classification for pGGO progression was proposed based on thin-section CT images obtained during the follow-up phase. The pGGOs of lung cancer nodules do not only increase in size or density, but may also decrease rapidly or slowly with the appearance of solid components. Close follow-up until the appearance of a solid component may be a valid option for the management of pGGO.

ACKNOWLEDGMENTS

The authors thank Fumio Shishido, MD, PhD (Department of Radiology, School of Medicine, Fukushima Medical University) for his encouragement. We also wish to thank the pathologists who assisted in this study: Yoshihiro Matsuno, MD (National Cancer Center Research Institute), Tomoyuki Yokose, MD, and Genichiro Ishii, MD (National Cancer Center Research Institute East). We also thank the physicians, the

technical staff, and the administrative staff of the Anti–Lung Cancer Association in Tokyo.

REFERENCES

1. Nakajima R, Yokose T, Kakinuma R, et al. Localized pure ground-glass opacity on high-resolution CT: histologic characteristics. *J Comput Assist Tomogr*. 2002;26:323–329.
2. Nakata M, Saeki H, Takata I, et al. Focal ground-glass opacity detected by low-dose helical CT. *Chest*. 2002;121:1464–1467.
3. Kuriyama K, Seto M, Kasugai T, et al. Ground-glass opacity on thin-section CT: value in differentiating subtypes of adenocarcinoma of the lung. *AJR Am J Roentgenol*. 1999;173:465–469.
4. Yang ZG, Sone S, Takashima S, et al. High-resolution CT analysis of small peripheral lung adenocarcinomas revealed on screening helical CT. *AJR Am J Roentgenol*. 2001;176:1399–1407.
5. Henschke CI, Yankelevitz DF, Mirtcheva R, et al. CT screening for lung cancer: frequency and significance of part-solid and nonsolid nodules. *AJR Am J Roentgenol*. 2002;178:1053–1057.
6. Kodama K, Higashiyama M, Yokouchi H, et al. Prognostic value of ground-glass opacity found in small lung adenocarcinoma on high-resolution CT scanning. *Lung Cancer*. 2001;33:17–25.
7. Kodama K, Higashiyama M, Yokouchi H, et al. Natural history of pure ground-glass opacity after long-term follow-up of more than 2 years. *Ann Thorac Surg*. 2002;73:386–393.
8. Suzuki K, Asamura H, Kusumoto M, et al. "Early" peripheral lung cancer: prognostic significance of ground-glass opacity on thin-section computed tomographic scan. *Ann Thorac Surg*. 2002;74:1635–1639.
9. Matsuguma H, Yokoi K, Anraku M, et al. Proportion of ground-glass opacity on high-resolution computed tomography in clinical T1N0M0 adenocarcinoma of the lung: a predictor of lymph node metastasis. *J Thorac Cardiovasc Surg*. 2002;124:278–284.
10. Kondo T, Yamada K, Noda K, et al. Radiologic-prognostic correlation in patients with small pulmonary adenocarcnomas. *Lung Cancer*. 2002;36: 49–57.
11. Austin JM, Muller NL, Friedman PJ, et al. Glossary of terms for CT of the lung: recommendations of the Nomenclature Committee of the Fleischner Society. *Radiology*. 1996;200:327–331.
12. Aoki T, Nakata H, Watanabe H, et al. Evolution of peripheral lung adenocarcinomas: CT findings correlated with histology and tumor doubling time. *AJR Am J Roentgenol*. 2000;174:763–768.
13. White CS, Romney BM, Mason AC, et al. Primary carcinoma of the lung overlooked at CT: analysis of findings in 14 patients. *Radiology*. 1996; 199:109–115.
14. Gurney JW. Missed lung cancer at CT: imaging findings in nine patients. *Radiology*. 1996;199:117–122.
15. Koizumi N, Sakai K, Matsuzuki Y, et al. Natural history of cloudy zone of pulmonary adenocarcinoma on HRCT [in Japanese]. *Nippon Igaku Hoshasen Gakkai Zasshi*. 1996;56:715–719.
16. Jang HJ, Lee KS, Kwon OJ, et al. Bronchioloalveolar carcinoma: focal area of ground-glass attenuation at thin-section CT as an early sign. *Radiology*. 1996;199:485–488.
17. Takashima S, Maruyama Y, Hasegawa M, et al. CT findings and progression of small peripheral lung neoplasms having a replacement growth pattern. *AJR Am J Roentgenol*. 2003;180:817–826.
18. Kakinuma R, Ohmatsu H, Kaneko M, et al. Detection failures in spiral CT screening for lung cancer: analysis of CT findings. *Radiology*. 1999;212: 61–66.
19. Li F, Sone S, Abe H, et al. Lung cancers missed at low-dose helical CT screening in a general population: comparison of clinical, histopathologic, and imaging findings. *Radiology*. 2002;225:673–683.
20. Kaneko M, Eguchi K, Ohmatsu H, et al. Peripheral lung cancer: screening and detection with low-dose spiral CT versus radiography. *Radiology*. 1996;201:798–802.
21. Sobue T, Moriyama N, Kaneko M, et al. Screening for lung cancer with low-dose helical computed tomography: Anti–Lung Cancer Association project. *J Clin Oncol*. 2002;20:911–920.
22. Schwartz M. A biomathematical approach to clinical tumor growth. *Cancer*. 1961;14:1272–1294.
23. Travis W, Colby T, Corrin B, et al. *Histological Typing of Lung and Pleural Tumors*. Berlin: Springer; 1999.
24. Noguchi M, Morikawa A, Kawasaki M, et al. Small adenocarcinoma of the lung: histologic characteristics and prognosis. *Cancer*. 1995;75:2844–2852.
25. Yankelevitz DF, Henschke CI. Does 2-year stability imply that pulmonary nodules are benign? *AJR Am J Roentgenol*. 1997;168:325–328.
26. Swensen SJ, Jett JR, Hartman TE, et al. Lung cancer screening with CT: Mayo Clinic experience. *Radiology*. 2003;226:756–761.
27. Benjamin MS, Drucker EA, McLoud TC, et al. Small pulmonary nodules: detection at chest CT and outcome. *Radiology*. 2003;226:489–493.
28. Hasegawa M, Sone S, Takashima S, et al. Growth rate of small lung cancers detected on mass CT screening. *Br J Radiol*. 2000;73:1252–1259.
29. Nakata M, Sawada S, Saeki H, et al. Prospective study of thoracoscopic limited resection for ground-glass opacity selected by computed tomography. *Ann Thorac Surg*. 2003;75:1601–1606.
30. Suzuki K, Yokose T, Yoshida J, et al. Prognostic significance of the size of central fibrosis in peripheral adenocarcinoma of the lung. *Ann Thorac Surg*. 2000;69:893–897.
31. Aoki T, Tomoda Y, Watanabe H, et al. Peripheral lung adenocarcinoma: correlation of thin-section CT findings with histologic prognostic factors and survival. *Radiology*. 2001;220:803–809.
32. Yankelevitz Df, Reeves AP, Kostis WJ, et al. Small pulmonary nodules: volumetrically determined growth rates based on CT evaluation. *Radiology*. 2000;217:251–256.
33. Ko JP, Rusinek H, Jacobs EL, et al. Small pulmonary nodules: volume measurement at chest CT-phantom study. *Radiology*. 2003;228:864–870.

Reprinted from
Jpn J Clin Oncol 2004;34(3)118–123

Magnetic Anchor for More Effective Endoscopic Mucosal Resection

Toshiaki Kobayashi[1], Takushi Gotohda[1], Katsunori Tamakawa[2], Hirohisa Ueda[3] and Tadao Kakizoe[1]

[1]National Cancer Center, Tokyo, [2]Tamakawa Corporation, Sendai, [3]Pentax Corporation, Tokyo, Japan

Jpn J Clin Oncol 2004;34(3)118–123

Magnetic Anchor for More Effective Endoscopic Mucosal Resection

Toshiaki Kobayashi[1], Takushi Gotohda[1], Katsunori Tamakawa[2], Hirohisa Ueda[3] and Tadao Kakizoe[1]

[1]National Cancer Center, Tokyo, [2]Tamakawa Corporation, Sendai, [3]Pentax Corporation, Tokyo, Japan

Received September 24, 2003; accepted January 16, 2004

Background: Technical difficulties are involved in endoscopic mucosal resection (EMR) of gastric cancer since it is a 'one handed surgery'. These difficulties prevent this technique from being indicated for larger lesions, even when it can possibly be performed for patients with such lesions. If microforceps could assist EMR, this procedure would become easier and safer. Since magnetic force can control objects without direct contact, it can be applied to control microforceps internally in assistance with EMR.

Methods: We developed a magnetic anchor consisting of three parts: a magnetic weight with dimensions of 1.0 × 1.0 × 1.5 cm, microforceps and a connecting thread. Endoscopic clips used in hemostasis were used as the microforceps of the magnetic anchor in this study. The magnetic control system consisted of a 0.68 kOe/10 cm/100 A electromagnet, 350 mm in diameter and a circumventing positional frame. The microforceps were inserted into a sheath within the endoscope, and the magnetic weight was secured to the tip of the sheath protruding from the endoscope. The magnetic anchor, along with the endoscope, was inserted through an overtube into the gastric cavity of a swine under general anesthesia. The magnetic anchor was used in a manner similar to that in standard surgery, and EMR was thereby performed.

Results: The mucosa to be resected was satisfactorily dragged and stabilized. The magnetic anchor facilitated EMR, regardless of the technical skills of the endoscopist and region of the stomach at which the technique was performed.

Conclusion: The magnetic anchor is considered to have alleviated some technical problems involved in EMR. It has the potential for making EMR a safer and quicker procedure for the treatment of early gastric cancer, when appropriately indicated.

Key words: endoscopic mucosal resection (EMR) – microforceps – magnetic anchor – gastric cancer – endoscopic surgery

INTRODUCTION

Endoscopic mucosal resection (EMR) of gastric cancer is a representative procedure of minimally invasive surgery (1). While this approach seems theoretically appropriate, it has serious problems especially when its indications are extended to lesions larger than those recommended by the Japanese Gastric Cancer Association (2). These problems arise from the fact that all resection procedures are carried out using only one endoscope. Thus, resection is performed without appropriate tissue tension provided by an assistant holding the tip of the mucosa. This 'one handed surgery' is the root cause of several problems, particularly when performing EMR on large lesions.

In EMR, the resection line cannot be fully observed because the ablated mucosa cannot be stabilized and pulled up. Consequently, it is difficult to make an accurate incision into the mucosa. Cutting of unconfirmed blood vessels causes bleeding, and hemostatic procedures are hindered because the bleeding point cannot be confirmed directly by operator's eyes. It is also of consequence that the depth of the mucosa at the site of ablation cannot be confirmed, which may lead to perforation of the gastric wall (1,3). These dilemmas have not caused serious problems so far, because EMR is indicated only for relatively small lesions.

Several new techniques and types of equipment have been developed to overcome these technical difficulties and complications that are problematic even for experienced endoscopists. The insulation-tipped electro-surgical knife (IT knife) is one such device that was designed by covering the tip of the electric knife with a ceramic ball to prevent accidental penetration of the gastric wall (1,4).

The rationale behind this development is that the tip of the electric knife, which is the most penetrative part for surgical incision, cannot be used. Thus, theoretically, resection is limited to a certain extent and the penetration is prevented.

For reprints and áll correspondence: Toshiaki Kobayashi, Cancer Screening Technology Division, Research Center for Cancer Prevention and Screening, National Cancer Center, 1-1, Tsukiji 5-chome, Chuo-ku, Tokyo 104-0045, Japan. E-mail: tkobayas@ncc.go.jp

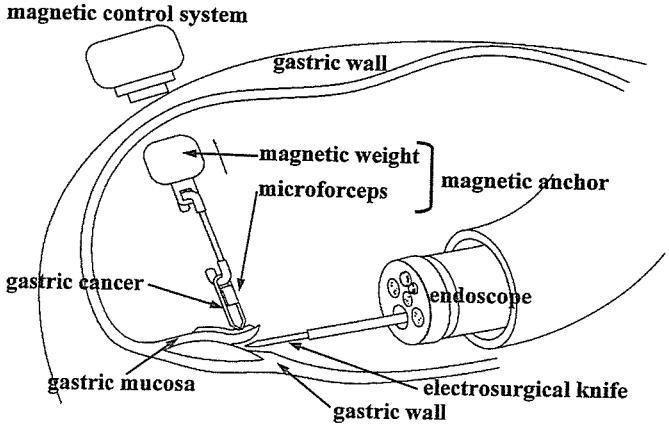

Figure 1. The concept of the magnetic anchor. The concept of the magnetic anchor is shown by microforceps that stabilize and pull up objects by employing a magnetic field. The magnetic anchor consists of three parts: microforceps, a magnetic weight and the connecting thread between them. One application of this concept is the use of the forceps to assist endoscopic resection of gastric cancer. The concept can even be applied to other procedures outside medical practice when stabilization and traction of objects are required and where direct contact is not possible.

However, perforation is still encountered, leading to prolonged resection time. Therefore, EMR for gastric cancer requires an endoscopist with technical skills higher than those required for other endoscopic procedures.

A basic technical principle of surgical resection is the resection of appropriate tissues, which are made to stand out by pulling them up. If this basic technique is integrated into EMR, then the procedure would become easier, less risky and more effective. This, in turn, could make it possible to establish EMR as the standard procedure whenever the nature of the lesions is an indication for resection with EMR, irrespective of their size.

Magnets and magnetic fields have been applied to catheter examinations to control the tips of catheters for years (5). They may also be providing a way to alter tissue contour configurations without any direct contact, such as through electric cables. A direct current magnetic field, as is used in MRI, is regarded as the least invasive, or even the most appropriate, non-invasive procedure that can be applied medically.

If a magnetic field is properly controlled and made to generate enough power to give sufficient force by using microforceps for stabilization of the mucosa during EMR (Fig. 1), then the procedure would be made much easier. If such a device design is developed, then indications for EMR could be expanded to change the current concept of endoscopic surgery for cancer treatment, including gastric cancer.

Thus, this study was initiated to evaluate the potential of magnetically controlled forceps and a magnetic anchor in an animal subject.

a. Positioning frame

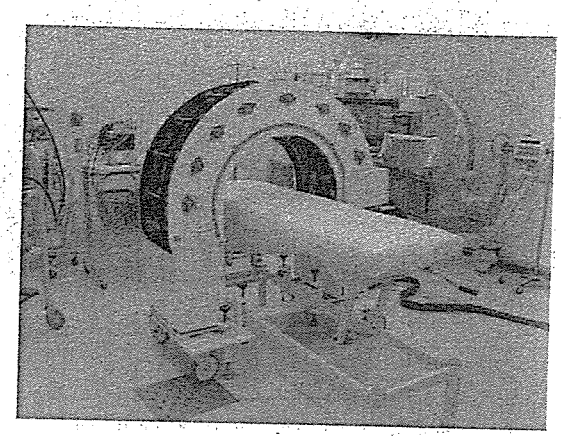

b. Electromagnet fixed to the belts

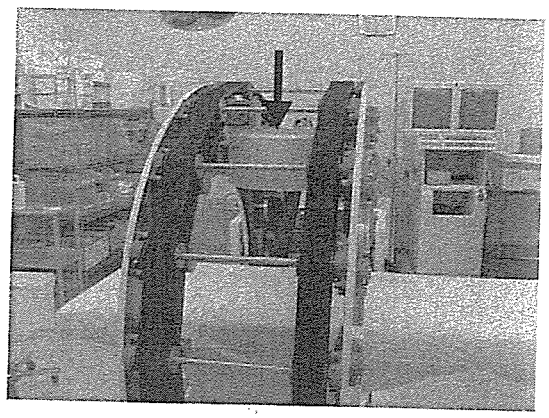

Figure 2. Magnetic control system. (a) Positioning frame: The positioning frame holds the electromagnet and allows its movement around the subject. Its wheels allow lateral movement along the table. (b) Electromagnet fixed to the belts: The electromagnet, shown by the arrow, is fixed to the belts that allow its movement around a subject inside the system. The electromagnet itself is compact; however, the frame is produced on a large scale to keep the distance between the subject and the electromagnet at a minimum.

SUBJECTS AND METHODS

MAGNETIC CONTROL SYSTEM

A magnetic control system was designed for clinical application in a standard endoscopic room, thus limiting the size of the system. The magnetic control system primarily consisted of a 0.68 kOe /100 A electromagnet, 350 mm in diameter, at 10 cm from the center of the magnetic yoke.

The electromagnet was fixed on belts contained in a semicircular positioning frame that revolved around the trails of the frame. In this manner, a pulley system was formed allowing a 180° control of the magnet's position in relation to the patient (Fig. 2).

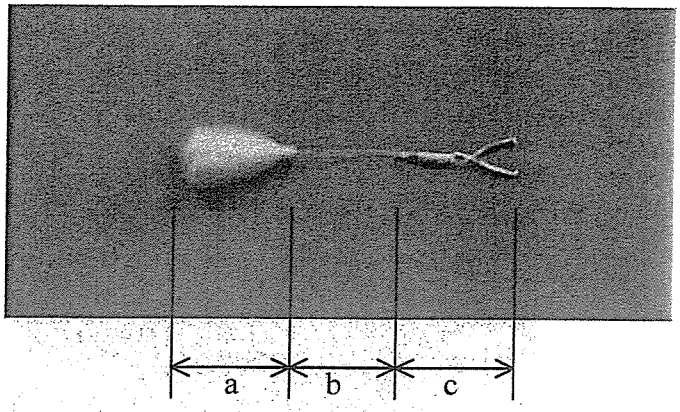

Figure 3. Magnetic anchor. The magnetic anchor consists of three parts: (a) a magnetic weight, (c) microforceps and (b) a thread connecting them.

MAGNETIC ANCHOR

The magnetic anchor consists of three parts: a hand-made magnetic weight comprising magnetic stainless steel (SUS420F), microforceps and a connecting thread (Fig. 3). The weight, with dimensions of 1.0 × 1.0 × 1.5 cm, was designed to generate sufficient traction for tissues and to allow insertion into the gastric cavity through the esophagus. The weight of the anchor can be varied by using differently shaped weight components of different weights. The anchor weight used for this procedure is approximately 6 g.

Hemostasis clips (endo-clips) were used as microforceps in order to confirm the feasibility of the magnetic anchor's proposed function of tissue traction. However, it is likely that forceps designed specially for this procedure will be developed in the future.

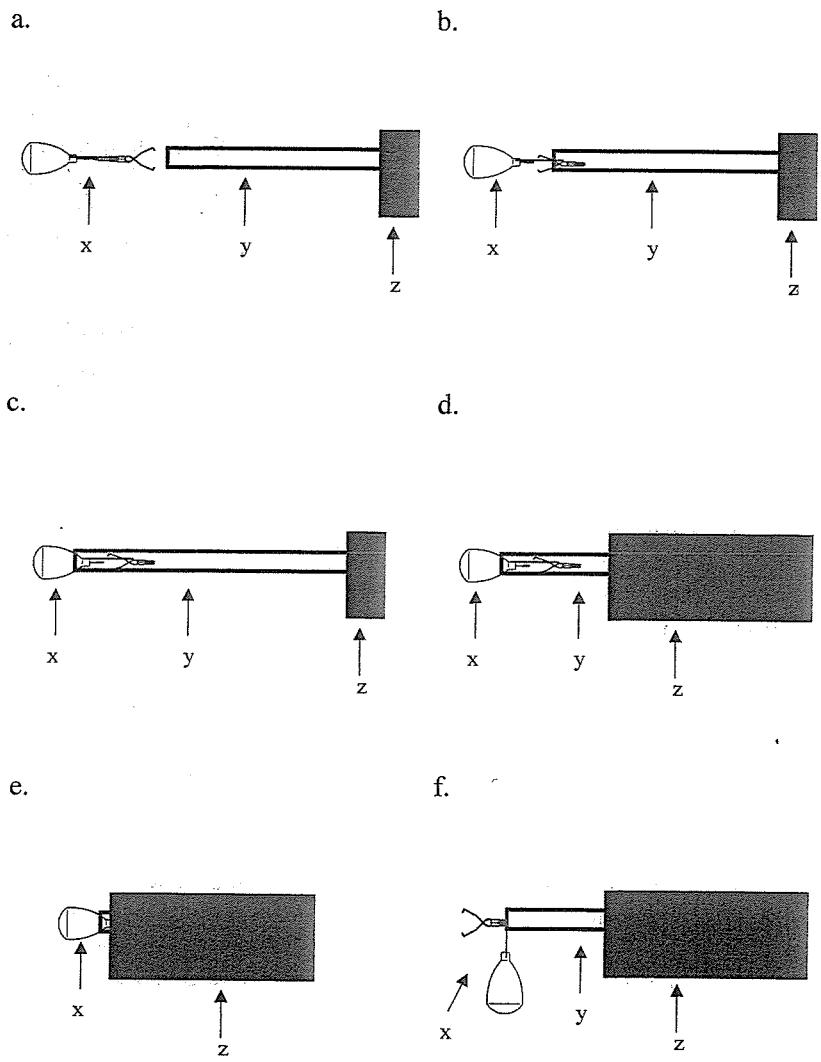

Figure 4. Preparation of the magnetic anchor. (a) The magnetic anchor (x) is prepared by the following procedure: First, the endoscopic hemostasis sheath (y) is inserted into the working channel of an endoscope (z) and pushed out from the tip of the endoscope. (b) The microforceps are connected to the sheath and pulled backwards into the sheath. (c) The thread is pulled further into the sheath together with the magnetic weight, and the magnetic weight is secured at the tip of the sheath. (d) The sheath is pulled into the endoscope. (e) The weight is fixed at the tip of the endoscope. (f) The magnetic anchor is pushed out from the tip of the endoscope at the time of its use. The target is grasped after opening the microforceps. x: magnetic anchor, y: endoscopic hemostasis sheath, z: endoscope.

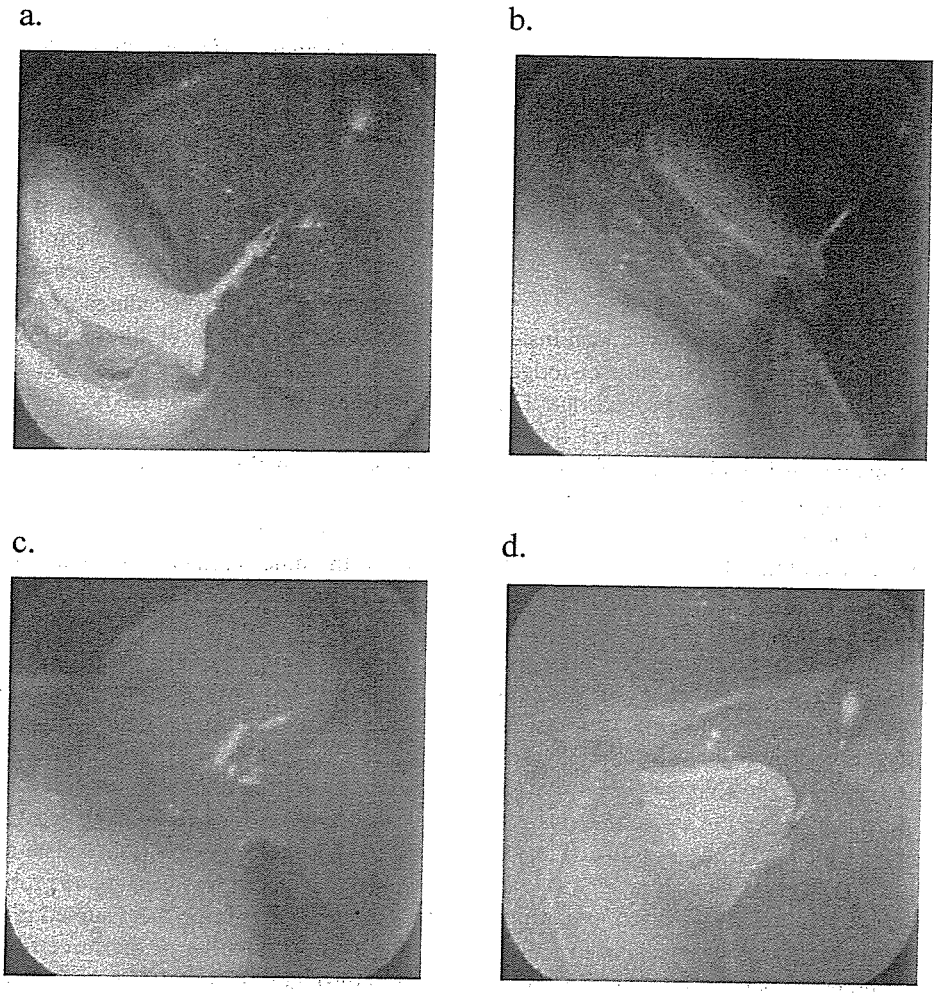

Figure 5. Resection using the magnetic anchor. (a) The mucosa is pulled to create sufficient space to show the line of resection. (b) The resection is performed using an electric knife through an endoscope. (c) The resection line can be clearly shown as a result of traction by the magnetic anchor. (d) The traction of the magnetic anchor is sufficient to allow the mucosal flap to be turned over.

Preparation of the Magnetic Anchor

First, the endoscopic hemostasis sheath is inserted into the working channel of an endoscope as shown in Fig. 4. The microforceps are then connected to the sheath and are pulled backwards into the tip of the sheath protruding from the tip of the endoscope; subsequently, the thread follows and the anchor is secured at the tip of the sheath. The sheath is then withdrawn into the working channel, and the anchor is fixed at the tip of the endoscope.

Test Subject

A 45 kg female swine laid in the left lateral position, was placed on an examination table under intravenous anesthesia.

Procedure

Prior to insertion of the magnetic anchor, an incision was made by the standard EMR technique in the mucosa surrounding the region of the stomach intended for resection (4). An overtube was first inserted into the esophagus to facilitate smooth insertion of the endoscope along with the magnetic anchor to reach the gastric cavity. Inside the gastric lumen, the magnetic weight was pushed out from the sheath, followed by the microforceps. The tip of the mucosa, in which the incision was made in advance, was grasped by the microforceps. In order to lift the tip of the mucosa, a magnetic field was then generated by increasing the electric current through the electromagnet of the magnetic control system.

The EMR procedure was performed by several physicians of the National Cancer Center Hospital at four representative regions of the stomach: the anterior wall of the gastric angle, the lesser curvature of the gastric corpus, the posterior wall of the gastric angle and the greater curvature of the gastric corpus. These areas were selected in order to represent the varying techniques and problems that are incurred with the anatomy of each specific area.

RESULTS

Insertion of the fixed magnetic anchor through the overtube incurred no difficulties. In fact, the magnetic anchor was easily

Table 1. Sizes of resected specimens and the procedure times required

Site in the stomach	Size (cm)	Time (min)
Anterior wall of the gastric angle	5.1 × 2.7	51
Lesser curvature of the gastric corpus	2.4 × 1.7	47
Posterior wall of the gastric angle	2.9 × 1.7	25
Greater curvature of the gastric corpus	9.4 × 5.1	73

introduced even without the overtube. Once introduced inside the gastric lumen, the magnetic weight smoothly dislodged from the sheath and the forceps were easily pushed out. The mucosal target site for traction was easily grasped by the microforceps in the same manner as in endoscopic hemostasis, despite the heaviness of the weight component of the anchor.

As a result of magnetic attraction, the magnetic anchor rose rapidly when the electric current of the electromagnet was sufficient for the operation, pulling up the mucosa in a stable tent-like form (Fig. 5). The direction of the traction for the magnetic anchor could be controlled simply by changing the position of the electromagnet over the animal. Application of magnetic attraction only from above was sufficient to pull the magnetic anchor in the desired direction. The control of the magnetic anchor could also be facilitated by adjusting the position of the swine and/or placing a spacer between the swine and the bed. Thus, the magnetic anchor pulled up the mucosa sufficiently to show the resection line. Moreover, hemorrhage was rare because blood vessels could be clearly visualized endoscopically, and electrocoagulation hemostatic procedures were conducted before cutting the blood vessels. Even on occasions of unexpected hemorrhage, hemostasis proved easier because the site of bleeding was clearly visible by stretching the mucosal folds using the magnetic anchor.

The basic features and functions of the magnetic anchor were similar at all the four tested representative areas of the stomach, and the magnetic anchor could be controlled in the same manner at all sites. Sizes of resected specimens and the procedure time required for each are shown in Table 1.

DISCUSSION

Conventional surgery for cancer is highly stressful and sometimes burdensome for patients. Standard treatment for gastric cancer at present is gastrectomy, which is performed even for early gastric cancer. One alternative to gastrectomy that has recently emerged is EMR, although it has several technical problems related to its one handed surgery approach. This procedure, in turn, demands additional skills that are beyond those required for a standard endoscopic technique.

However, the magnetic anchor is not a technique in itself but just an additional tool which is optionally used by the endoscopist during EMR. In the present experiment, endoscopists used the magnetic anchor throughout the procedure and found that EMR was much easier by using it. This opinion was unanimous even on their first exposure to the new device. The magnetic anchor facilitated resection even with the techniques used for standard EMR, which are different from those used for standard surgery. It is worth noting that it was not necessary for the endoscopists to modify their technique in using the magnetic anchor. In fact, they found that the use of the anchor offered more benefits.

The first EMR procedure using the magnetic anchor was performed by a senior physician, the following two by resident physicians, and the last one by a senior physician with a resident physician. All the procedures were performed with few or no incidents regardless of the skills of the physicians. The senior physician, who has developed skills for using the IT knife, had to modify technique he used for standard surgery in order to maximize the efficacy of the magnetic anchor. However, he did not find it difficult. Even for resident physicians inexperienced with an IT knife, EMR with the magnetic anchor proved easy to perform. According to the endoscopists, one touch to the mucosa made it sufficient for cutting. This was a great contrast to the frustration that they had when performing standard EMR without the magnetic anchor, which demanded much effort and patience.

However, several noteworthy incidents had occurred during the procedure. Prominent among them were separation of the magnetic weight from the thread connecting the forceps and slipping of the microforceps from the mucosa. In these cases, new magnetic anchors could be inserted without any problems, and the procedure was continued. The malfunctioned anchors could be easily removed causing no problem, even when left in the gastric lumen during the resumed resection procedure with a new anchor. Slipping of the forceps occurred twice for the same physician at the same mucosal site. Thus, this may be attributed to his inexperience in surgical techniques, which would be similar to the problems encountered with some assistants in standard surgery. Of greater importance was the unproblematic retrieval of the dislodged magnetic anchor. In fact, one of the reasons for involving various physicians in this experiment was to evaluate the nature of incidents with the device and to consider possible countermeasures for future improvement. Thus, the magnetic anchor will certainly be improved, and refined, and will present with few benign problems that we expect to overcome easily. We emphasize that the magnetic anchors used in this study were merely handmade ones devised to experimentally assess the conceptual feasibility of the technique.

Problems with standard EMR such as perforation and incomplete resection are serious and potentially hinder the EMR procedure from being indicated to lesions proposed for resection by the National Cancer Center Hospital of Japan. Even though indications for EMR procedures may be discussed in later papers, we believe that several current problems with EMR are solved to a great extent by the use of the magnetic anchor.

The results of this study showed that all procedures were satisfactorily performed using an electric current of less than 50 A for the electromagnet, which is comparable to 0.6 kOe/1.0 cm. Consequently, the intensity of the magnetic field required for

the magnetic anchor for EMR was less than what had been expected prior to this procedure. Our next model of the magnetic control system will be smaller and simpler. New concepts of magnetic anchor will expand the indications of endoscopic surgery beyond the treatment of gastric cancer.

Acknowledgments

This study was supported by a Grant-in-Aid for the Research on Advanced Medical Technology of the Ministry of Health, Labor and Welfare, and a Grant-in-Aid for the Second Term Comprehensive 10-year Strategy for Cancer Control, of the Ministry of Health, Labor and Welfare. The authors thank Professor J. Patrick Barron of the International Medical Communication Center, Tokyo Medical University, for his review of the manuscript, and Professor Ken-ichi Arai of Tohoku University for his technical advice.

References

1. Rembacken BJ, Gotoda T, Fujii T, Axon ATR. Endoscopic mucosal resection. *Endoscopy* 2001;33(8):709–18.
2. Gotoda T, Yanagisawa A, Sasako M, Ono H, Nakanishi Y, Shimoda T, et al. Incidence of lymph node metastasis from early gastric cancer: estimation with a large number of cases at two large centers. *Gastric Cancer* 2000;3:219–25.
3. Tada M. One piece resection and piecemeal resection of early gastric cancer by strip biopsy. *Igakushoin* 1998;68–87 (in Japanese).
4. Gotoda T, Kondo H, Ono H, Saito Y, Yamaguchi H, Saito D, et al. A new endoscopic mucosal resection procedure using an insulation-tipped electrosurgical knife for rectal flat lesions: report of two cases. *Gastrointest Endosc* 1999;50:560–3.
5. Faddis MN, Blume W, Finney J, Hall A, Rauch J, Sell J, et al. Novel, magnetically guided catheter for endocardial mapping and radiofrequency catheter ablation. *Circulation* 2002;106:2980–5.

Fluorine 18–tagged fluorodeoxyglucose positron emission tomographic scanning to predict lymph node metastasis, invasiveness, or both, in clinical T1 N0 M0 lung adenocarcinoma

Hiroaki Nomori, MD, PhD[a]
Kenichi Watanabe, MD[a]
Takashi Ohtsuka, MD[a]
Tsuguo Naruke, MD, PhD[a]
Keiichi Suemasu, MD, PhD[a]
Toshiaki Kobayashi, MD, PhD[b]
Kimiichi Uno, MD, PhD[c]

See related editorial on page 341.

Objective: We sought to predict lymph node metastasis and tumor invasiveness in clinical T1 N0 M0 lung adenocarcinomas, and we measured fluorodeoxyglucose uptake on positron emission tomography.

Methods: Fluorodeoxyglucose positron emission tomography was performed on 44 patients with adenocarcinomas of 1 to 3 cm in size clinically staged as T1 N0 M0 before major lung resection with lymph node dissection. Fluorodeoxyglucose uptake was evaluated by using the contrast ratio between the tumor and contralateral healthy lung tissue. Lymphatic and vascular invasion within tumors, pleural involvement, and grade of histologic differentiation were examined.

Results: The pathologic tumor stage was T1 N0 M0 in 36 patients, and a more advanced stage was found in 8 patients. Although all 22 adenocarcinomas with a contrast ratio of less than 0.5 in fluorodeoxyglucose uptake were pathologic T1 N0 M0 tumors, 8 (36%) of 22 with a contrast ratio of 0.5 or greater were of a more advanced stage than T1 N0 M0, with the difference being significant ($P = .002$). Adenocarcinomas with a contrast ratio of less than 0.5 showed less lymphatic and vascular invasion and less pleural involvement than those with a contrast ratio of 0.5 or greater ($P = .006$, $P = .004$, and $P = .02$, respectively). The grade of histologic differentiation was well differentiated in 19 of 22 adenocarcinomas with a contrast ratio of less than 0.5 (86%), which was a greater frequency than the 4 (18%) of 22 adenocarcinomas with a contrast ratio of 0.5 or greater ($P < .001$).

Conclusion: Clinical T1 N0 M0 lung adenocarcinomas with a contrast ratio of less than 0.5 usually did not have lymph node metastasis, had less tumor involvement of vessels or pleura, and were more frequently well differentiated than those with a contrast ratio of 0.5 or greater. Limited lung resection could be indicated, lymph node dissection or mediastinoscopy could be reduced, or both in this type of adenocarcinoma.

From the Department of Thoracic Surgery,[a] Saiseikai Central Hospital, Tokyo, Japan; the Endoscopy Division,[b] National Cancer Center Hospital, Tokyo, Japan; and Nishidai Clinic,[c] Tokyo, Japan.

This work was supported in part by a Grant-in-Aid from the Ministry of Health, Labor, and Welfare of Japan.

Received for publication Dec 17, 2003; revisions requested Feb 12, 2004; accepted for publication March 22, 2004.

Address for reprints: Hiroaki Nomori, MD, PhD, Department of Thoracic Surgery, Saiseikai Central Hospital, 1-4-17 Mita, Minato-ku, Tokyo 108-0073, Japan (E-mail: hnomori@qk9.so-net.ne.jp).

J Thorac Cardiovasc Surg 2004;128: 396-401

0022-5223/$30.00

doi:10.1016/j.jtcvs.2004.03.020

Recent advances in low-dose helical computed tomography (CT) and video-assisted thoracoscopic surgery have enabled the diagnosis of lung cancers while still small in size.[1-6] Although limited resection procedures, such as lung wedge resection or segmentectomy, can cure some clinical T1 N0 M0 non–small cell lung cancers (NSCLCs),[7,8] lymph node metastases are still found in approximately 20% of clinical T1 N0 M0 lung adenocarcinomas.[9-11] Even for patients with pathologic T1 N0 M0 NSCLCs, tumor involvement of intratumoral vessels or the pleura can also cause local recurrence after limited resection because of the spread of tumor cells into lymphatic vessels outside the primary tumor. To predict which T1 N0 M0 lung adenocarcinomas are curable with limited resection from CT findings, several reports have evaluated the importance of ground-glass opacity (GGO) within tumors, usually indicating bronchioloalveolar carcinoma–like spread because adenocarcinomas with GGO appearance are more frequently N0 stage and have less tumor involvement of intratumoral vessels or pleura than those with a solid appearance.[12,13] The criteria of defining GGO appearance on CT scans are subjective, however, potentially leading to erroneous selection of limited surgical intervention.

In recent years, fluorodeoxyglucose (FDG) positron emission tomography (PET) has been used to evaluate pulmonary nodules and tumor stages. It has been reported that FDG uptake correlates with the proliferative activity of tumors[14,15] and is an independent prognostic factor,[16,17] particularly in lung adenocarcinoma. The prognosis in lung adenocarcinoma is known to depend on not only tumor stage but also tumor involvement of intratumoral vessels or pleura.[9,10,18] To predict lymph node metastases and tumor involvement of intratumoral vessels or pleura in clinical T1 N0 M0 lung adenocarcinomas, we measured FDG uptake to determine any correlation with lymph node metastases, lymphatic and vascular invasion, and pleural involvement.

Materials and Methods

Patients

From December 2001 through October 2003, prospective FDG-PET and CT scans were performed for 223 noncalcified pulmonary nodules. Of these, 93 nodules were malignant tumors less than 3 cm in diameter on CT. Clinical TNM stage was determined by using both CT and PET scanning. Of the 93 malignant nodules, 48 were clinical T1 N0 M0 adenocarcinomas of the lung, and these underwent major lung resection with mediastinal lymph node dissection. We excluded 4 adenocarcinomas less than 1 cm in diameter that were PET negative because the spatial resolution of the current generation of PET scanners is 0.7 to 0.8 cm, making it difficult to image pulmonary nodules of less than 1 cm. As a result, we studied 44 adenocarcinomas that were clinically staged as T1 N0 M0 of sizes from 1 to 3 cm. The medical record of each patient was examined with regard to age, sex, maximum tumor diameter, serum level of carcinoembryonic antigen (CEA; <5 ng/mL vs ≥5 ng/mL), operative procedure, pathologic TNM stage, vascular or lymphatic invasion within tumors (positive vs negative), pleural involvement (p0 vs p1 to p3), and grade of histologic differentiation. To identify tumor involvement of the intratumoral vessels or pleura, we routinely conducted elastica-van Gieson staining. Pleural involvement was classified as p0, p1, p2, or p3; that is, a p0 tumor did not extend beyond the elastic pleural layer, a p1 tumor invaded the visceral pleural elastic layer but did not reach the pleural surface, a p2 tumor included tumor exposure on the pleural surface, and a p3 tumor invaded the parietal pleura or chest wall. The tumor stages were based on the TNM classification of the International Union Against Cancer[19]: p2 tumors were classified as T2; p3 tumors were classified as T3; and tumors with intrapulmonary metastasis within the same lobe were classified as T4. Grades of histologic differentiation were classified as well, moderately, or poorly differentiated.

FDG-PET Scanning

Patients were instructed to fast for at least 4 hours before intravenous administration of fluorine 18–tagged FDG. The dosage of fluorine 18–tagged FDG administered was 125 μCi/kg (4.6 MBq/kg) of body weight for nondiabetic patients and 150 μCi/kg (5.6 MBq/kg) of body weight for diabetic patients. PET imaging was performed approximately 60 minutes after administration of FDG with a POSICAM.HZL mPOWER (Positron Co, Houston, Tex). No-attenuation-corrected emission scans were initially obtained in 2-dimensional, high-sensitivity mode for 4 minutes per bed position and taken from the vertical skull through to the midthighs. Immediately thereafter, a 2-bed-position attenuation-corrected examination was performed, with 6 minutes for the emission sequence and 6 minutes for the transmission sequence at each bed position. The images were usually reconstructed in a 256 × 256 matrix by using ordered subset expectation maximization corresponding to a pixel size of 4 × 4 mm, with section spacing of 2.66 mm.

PET Data Analysis

The FDG-PET data were evaluated semiquantitatively on the basis of the contrast ratio (CR) obtained as follows. The regions of interest (ROIs) were placed in the nodules and contralateral lung. Highest activities in the tumor ROI (T) and in the contralateral normal lung ROI (N) were measured. The CR was calculated by using the formula $(T - N)/(T + N)$ in each nodule as an index of FDG uptake. After correction for radioactive decay, the ROIs were also analyzed by computing the standard uptake value (SUV), which was calculated on the basis of the following equation: Tumor activity concentration/Injected dose/Body weight. The maximum SUV within the selected ROIs was also measured and compared with the results of CR.

Statistical Analysis

All data were analyzed for significance by using the 2-tailed Student t test. All values in the text and tables are given as means ± SD.

TABLE 1. Tumor involvements and pathologic TNM stage for each CR value

CR of FDG uptake	Total lesions	>T1 N0 M0*	Lymphatic invasion	Vascular invasion	Pleural involvement
0.3	16	0	5	1	1
0.4	19	0	5	1	1
0.5†	22	0	5	1	1
0.6	29	2	9	2	2
0.7	37	4	14	7	6
0.8	39	4	15	8	6
0.9	43	8	19	10	8
1.0	44	8	19	10	8

*Pathologically more advanced stages than T1 N0 M0. Three of the 8 cases were p2; the other 5 were p1.
†Cutoff value of CR.

TABLE 2. PET findings and patients' characteristics, tumor size, and serum level of CEA

	CR of FDG uptake		P
	<0.5 (n = 22)	≥0.5 (n = 22)	value
Age (y, mean ± SD)	63 ± 11	64 ± 13	NS
Male (No.)	14	10	NS
Female (No.)	8	12	
Tumor size (cm, mean ± SD)	1.9 ± 0.6	2.2 ± 0.4	NS
CEA (ng/mL)			.001
<5.0	22	10	
≥5.0	0	12	

NS, Not statistically significant.

TABLE 3. Correlation between PET findings and pathologic tumor stage

		CR of FDG uptake	
Pathologic TNM	Total (n = 44)	<0.5 (n = 22)	≥0.5 (n = 22)
T1 N0 M0	36	22*	14*
T1 N1 M0	3	0	3
T2 N0 M0	3	0	3
T4 N0 M0	2	0	2

T2 is classified from pleural involvement grade, p2. T4 is classified from intrapulmonary metastasis.
*Significant difference in the frequency of T1 N0 M0 between the CR <0.5 and CR ≥0.5 groups ($P = .002$).

Results

The pathologic tumor stage was T1 N0 M0 in 36 patients and more advanced in 8 patients (ie, T1 N1 M0 in 3 patients, T2 N0 M0 in 3 patients, and T4 N0 M0 in 2 patients). Lymphatic or vascular invasion within tumors and pleural involvement was seen in 19, 10, and 8 patients, respectively. Table 1 shows the various CR values with relation to the pathologic tumor stage, lymphatic and vascular invasion, and pleural involvement. Although all adenocarcinomas with a CR of less than 0.5 were pathologically staged as T1 N0 M0, some adenocarcinomas with a CR of 0.5 or greater were more advanced than T1 N0 M0, with more frequent lymphatic and vascular invasion and pleural involvement than the former. Therefore medical records were compared between the 22 adenocarcinomas with a CR of less than 0.5 and the 22 adenocarcinomas with a CR of 0.5 or greater.

The maximum SUVs ranged from 0.5 to 3.1 (mean, 1.1 ± 0.7) in the 22 adenocarcinomas with a CR of less than 0.5 and from 1.9 to 8.5 (mean, 3.9 ± 1.8) in the 22 adenocarcinomas with CRs of 0.5 or greater, with the difference between the 2 groups being significant ($P < .001$). Two (9%) of the 22 adenocarcinomas with CRs of less than 0.5 showed an SUV of 2.5 or greater, however, both of which were pathologically staged as T1 N0 M0 and had no involvements of intratumoral vessels or pleura. Seven (32%) of the 22 adenocarcinomas with CRs of 0.5 or greater had SUVs of less than 2.5, of which 2 had a more advanced tumor stage than T1 N0 M0, 6 had lymphatic invasion, and 1 had vascular invasion.

Table 2 shows the results of PET findings with patients' characteristics, tumor size, and serum level of CEA. None of the adenocarcinomas with CRs of less than 0.5 had increased serum levels of CEA, which was significantly less frequent than the incidence of increased CEA in the 12 (55%) of 22 adenocarcinomas with CRs of 0.5 or greater ($P < .001$). There was no significant difference between the 2 groups in mean age, sex ratio, or tumor size.

Table 3 shows the correlation between PET findings and pathologic tumor stage. All adenocarcinomas (100%) with CRs of less than 0.5 were staged as T1 N0 M0. Adenocarcinomas with CRs of 0.5 or greater were staged as T1 N0 M0 in 14 (64%) patients, T1 N1 M0 in 3 patients, T2 N0 M0 caused by p2 (tumor exposure on the pleural surface) in 3 patients, and T4 N0 M0 caused by intrapulmonary metastases in 2 patients. Adenocarcinomas with CRs of less than 0.5 were more likely to be pathologic T1 N0 M0 stage than those with CRs of 0.5 or greater ($P = .002$).

Table 4 shows the correlation between PET findings and lymphatic and vascular invasion within tumors and pleural involvement. Lymphatic invasion was seen in 5 (23%) of 22 adenocarcinomas with CRs of less than 0.5, which was significantly less frequent than 14 (64%) of 22 with CRs of 0.5 or greater ($P = .006$). Vascular invasion was seen in 1 (5%) of 22 adenocarcinomas with CRs of less than 0.5, which was significantly less frequent than 9 (41%) of 22 with CRs of 0.5 or greater ($P = .004$). Pleural involvement was seen in 1 (5%) of 22 adenocarcinomas with CRs of less than 0.5, which was significantly less frequent than 7 (32%) of 22 with CRs of 0.5 or greater ($P = .02$).

Table 5 shows the correlation between PET findings and the histologic degree of differentiation. In the adenocarcinomas with CRs of less than 0.5, well-differentiated and

TABLE 4. Correlation between PET findings and tumor involvement into intratumoral vessels or pleura

Tumor involvement	CR of FDG uptake		*P* value
	<0.5 (n = 22)	≥0.5 (n = 22)	
Lymphatic invasion			.006
Yes	5	14	
No	17	8	
Vascular invasion			.004
Yes	1	9	
No	21	13	
Pleural involvement			.02
p0	21	15	
p1-p2	1	7	

TABLE 5. Correlation between PET findings and grade of histologic differentiation of adenocarcinomas

Grade of differentiation	Total (n = 44)	CR of FDG uptake <0.5 (n = 22)	CR of FDG uptake ≥0.5 (n = 22)
Well differentiated	23	19*	4*
Moderately differentiated	17	3	14
Poorly differentiated	4	0	4

There was significant difference in frequency of well-differentiated adenocarcinomas between the CR <0.5 and CR ≥0.5 groups ($P < .001$).

TABLE 6. Correlation between PET findings and tumor stages, tumor involvement of intratumoral vessels, and tumor involvement of pleura in well-differentiated adenocarcinomas

Tumor stage and invasiveness	CR of FDG uptake >0.5 (n = 19)	CR of FDG uptake ≥0.5 (n = 4)	*P* value
TNM stage			<.01
T1 N0 M0	19	2	
>T1 N0 M0	0	2	
Lymphatic invasion			<.001
Yes	3	4	
No	16	0	
Vascular invasion			.02
Yes	1	2	
No	18	2	
Pleural involvement			<.01
p0	19	2	
p1-p2	0	2	

moderately differentiated adenocarcinomas were seen in 19 and 3 patients, respectively. In the adenocarcinomas with CRs of 0.5 or greater, well-differentiated, moderately differentiated, and poorly differentiated adenocarcinomas were seen in 4, 14, and 4 patients, respectively. Adenocarcinomas with CRs of less than 0.5 were more commonly well differentiated than those with CRs of 0.5 or greater ($P < .001$).

Table 6 shows the PET findings in well-differentiated adenocarcinomas with relation to the tumor stages and tumor involvements. Of the 4 well-differentiated adenocarcinomas with CRs of 0.5 or greater, each one (25%) was a pathologic T1 N1 M0 and T4 N0 M0 carcinoma, respectively; 4 (100%) had lymphatic invasion; 2 (50%) had vascular invasion; and 2 (50%) had pleural involvement. The well-differentiated adenocarcinomas with CRs of 0.5 or greater had advanced tumor stages, lymphatic and vascular invasion, and pleural involvement more frequently than those with CRs of less than 0.5 ($P < .01$, $P < .001$, $P = .02$, and $P < .01$, respectively).

Discussion

Although a criterion for diagnosing pulmonary malignancy with FDG-PET has frequently used an SUV with a cutoff value of 2.5,[20] some authors used visual evaluation, such as comparison of FDG uptake between nodules and mediastinal uptake.[21] The present study evaluated FDG uptake with CR instead of SUV for the following reasons: (1)hyperglycemia in diabetic patients decreases both the blood clearance of FDG and the accumulation of FDG in tumor tissue, and (2) SUV could be different between fat and thin patients because it is measured by using a body weight. Actually, the mean SUV of malignant pulmonary nodules has been reported to be various, ranging from 5.5 to 10.1.[22-25] In breast cancer, Wahl and coworkers[26] have demonstrated that a CR between tumor and contralateral normal breast is a reliable indicator for diagnosing malignancy. We accordingly used CR in the present study and determined that the cutoff value to differentiate between aggressive and nonaggressive adenocarcinomas was 0.5, with which we could differentiate the degree of tumor aggressiveness more accurately than with SUV.

The important points of the present study are as follows. Compared with adenocarcinomas with CRs of 0.5 or greater, those with CRs of less than 0.5 (1) did not show an increased serum level of CEA, (2) did not have lymph node metastases, (3) had less tumor involvement of vessels or pleura, and (4) were more frequently well-differentiated adenocarcinomas. The serum level of CEA in lung adenocarcinomas has been reported to be higher in N1 or N2 disease than in N0 disease.[27] FDG uptake in lung adenocarcinomas is known to often be negative in well-differentiated adenocarcinomas.[28] It has been also reported that well-differentiated adenocarcinomas are more commonly N0 stage and have less tumor involvement of vessels or pleura than moderately or poorly differentiated lesions.[9,12,13,18] Our results agree with those of these earlier studies. There were, however, 4 well-differentiated adenocarcinomas with CRs of 0.5 or greater that had more tumor aggressiveness than the 19 well-differentiated lesions with CRs of less than 0.5. We therefore consider that an FDG

uptake on PET can predict lymph node metastases and tumor invasiveness more accurately than the grade of histologic differentiation in clinical T1 N0 M0 adenocarcinomas.

Although limited resection could be a reasonable approach for T1 N0 M0 lung cancers, it has been reported that lymph node metastases are found in about 20% of clinical T1 N0 M0 adenocarcinomas.[9-11] In 1995, the Lung Cancer Study Group reported the results of a randomized control trial comparing limited resection and lobectomy for clinical T1 N0 M0 NSCLCs.[29] This trial demonstrated the inferiority of limited resection in terms of local relapse and prognosis because some patients actually had pathologic N1 or N2 disease. This is also because tumor involvement of intratumoral vessels or the pleura can cause local recurrence after limited resection, even for pathologic N0 disease, because of the spread of tumor cells into lymphatic vessels outside the primary tumor.[30] The present study showed that clinical T1 N0 M0 adenocarcinomas with CRs of less than 0.5 usually did not metastasize to the lymph nodes and seldom invaded the intratumoral vessels or pleura. This type of lung adenocarcinoma can be cured by means of limited surgical resection, such as segmentectomy or wedge resection. Although it has been reported that NSCLCs of less than 2 cm in size can be cured by means of segmentectomy with mediastinal lymph node dissection (ie, extended segmentectomy),[7] the indication of the extended segmentectomy could be expanded for adenocarcinomas with CRs of less than 0.5 that are less than 3 cm in size.

Mediastinal lymph node dissection is a useful procedure to secure complete local control of an NSCLC, with a subsequent improvement in both survival and nodal staging.[11] However, to minimize the damage caused by mediastinal node dissection in the patients with clinical stage I NSCLC, several authors reduced the dissection of some mediastinal lymph nodal stations with respect to the location of the primary tumor (ie, that the inferior and superior mediastinal lymph node stations could be reduced in the upper lobectomy and lower lobectomy, respectively).[31,32] To expand the possibility of reduction of mediastinal lymph node dissection, a successful intraoperative sentinel lymph node biopsy has been reported.[33,34] The present study showed that lymph node dissection could be reduced for clinical T1 N0 M0 adenocarcinomas with CRs of less than 0.5, without using the sentinel lymph node biopsy.

Although FDG-PET is well known to be useful for tumor staging in lung cancer, we believe that it can also predict lymph node metastases and tumor invasiveness in clinical T1 N0 M0 lung adenocarcinomas. Limited lung resection could be indicated, lymph node dissection or mediastinoscopy could be reduced, or both in this type of adenocarcinoma.

References

1. Kaneko M, Eguchi K, Ohmatsu H, et al. Peripheral lung cancer: screening and detection with low-dose spiral CT versus radiography. *Radiology*. 1996;201:798-802.
2. Yankelevitz DF, Gupta R, Zhao B, Henschke CI. Small pulmonary nodules: evaluation with repeat CT-preliminary experience. *Radiology*. 1999;212:561-6.
3. Henschke CI, Yankelevitz DF. CT screening for lung cancer. *Radiol Clin North Am*. 2000;38:487-95.
4. Nomori H, Horio H, Fuyuno G, Kobayashi R, Morinaga S, Suemasu K. Lung adenocarcinomas diagnosed by open or thoracoscopic vs. bronchoscopic biopsy. *Chest*. 1998;114:40-4.
5. Nomori H, Horio H. Colored collagen is a long-lasting point marker for small pulmonary nodules in thoracoscopic operations. *Ann Thorac Surg*. 1996;61:1070-3.
6. Nomori H, Horio H, Naruke T, Suemasu K. Fluoroscopy-assisted thoracoscopic resection of lung nodules marked with lipiodol. *Ann Thorac Surg*. 2002;74:170-3.
7. Yoshikawa K, Tsubota N, Kodama K, Ayabe H, Taki T, Mori T. Prospective study of extended segmentectomy for small lung tumors. *Ann Thorac Surg*. 2002;73:1055-9.
8. Kodama K, Doi O, Higashiyama M, Yokouchi H. Intentional limited resection for selected patients with T1 N0 M0 non-small cell lung cancer. *J Thorac Cardiovasc Surg*. 1997;114:347-53.
9. Suzuki K, Nagai K, Yoshida J, Nishimura M, Nishizaki Y. Predictors of lymph node and intrapulmonary metastasis in clinical stage IA non-small cell lung carcinoma. *Ann Thorac Surg*. 2001;72:352-6.
10. Asamura H, Nakayama H, Kondo H, Tsuchiya R, Shimosato Y, Naruke T. Lymph node involvement, recurrence, and prognosis in resected small, peripheral, non-small cell lung carcinomas: are these carcinomas candidates for video-assisted lobectomy? *J Thorac Cardiovasc Surg*. 1996;111:1125-34.
11. Naruke T, Goya T, Tsuchiya R, Suemasu K. The importance of surgery of non-small cell carcinoma of lung with mediastinal lymph node metastasis. *Ann Thorac Surg*. 1998;46:603-10.
12. Suzuki K, Asamura H, Kusumoto M, Kondo H, Tsuchiya R. Early peripheral lung cancer: prognostic significance of ground glass opacity on thin-section computed tomographic scan. *Ann Thorac Surg*. 2002; 74:1635-9.
13. Matsuguma H, Yokoi K, Anraku M, et al. Proportion of ground-glass opacity on high-resolution computed tomography in clinical T1 N0 M0 adenocarcinoma of the lung: a predictor of lymph node metastasis. *J Thorac Cardiovasc Surg*. 2002;124:278-84.
14. Higashi K, Ueda Y, Yagishita M, et al. FEG PET measurement of the proliferative potential of non-small cell lung cancer. *J Nucl Med*. 2000;41:85-92.
15. Vesselle H, Schmidt RA, Pugsley JM, et al. Lung cancer proliferation correlates with [F-18]fluorodeoxyglucose uptake by positron emission tomography. *Clin Cancer Res*. 2000;6:3837-44.
16. Ahuja V, Coleman RE, Herndon J, Patz EF. The prognostic significance of fluorodeoxyglucose positron emission tomography imaging for patients with non-small cell lung carcinoma. *Cancer*. 1998;83:918-24.
17. Vansteenkiste JF, Stroobants SG, Dupont PJ, et al. Prognostic importance of the standardized uptake value on ^{18}F-fluoro-2-deoxy-glucose-positron emission tomography in non-small cell lung cancer: an analysis of 125 cases. *J Clin Oncol*. 1999;17:3201-6.
18. Noguchi M, Morikawa A, Kawasaki M, et al. Small adenocarcinoma of the lung. Histologic characteristics and prognosis. *Cancer*. 1995; 75:2844-52.
19. Sobin LH, Wittekind Ch, editors. UICC: TNM classification of malignant tumours. 6th ed. New York: John Wiley & Sons; 2002. p. 99-103.
20. Coleman RE. PET in lung cancer. *J Nucl Med*. 1999;40:814-20.
21. Marom EM, Sarvis S, Herndon JE, et al. T1 lung cancers: sensitivity of diagnosis with fluorodeoxyglucose PET. *Radiology*. 2002;223: 453-9.
22. Dewan NA, Gupta NC, Redepenning LS, et al. Diagnostic efficacy of PET-FDG imaging in solitary pulmonary nodules. *Chest*. 1993;104: 997-1002.
23. Gupta NC, Maloof J, Gunel E. Probability of malignancy in solitary